



1 Sudden changes in nitrogen dioxide emissions over Greece 2 due to lockdown after the outbreak of COVID-19

3 Maria-Elissavet Koukouli^{1*}, Ioanna Skoulidou¹, Andreas Karavias², Isaak Parcharidis², Dimitris Balis¹, Astrid
4 Manders³, Arjo Segers³, Henk Eskes⁴ and Jos van Geffen⁴

5 ¹ Laboratory of Atmospheric Physics, Aristotle University of Thessaloniki, Greece.

6 ² Department of Geography, Harokopio University, Athens, Greece.

7 ³ TNO, Climate, Air and Sustainability, Utrecht, The Netherlands.

8 ⁴ Royal Netherlands Meteorological Institute (KNMI), De Bilt, The Netherlands.

9 * Correspondence: mariliza@auth.gr

10 **Abstract:** The unprecedented order, in modern peaceful times, for near-total lockdown of the Greek population,
11 as means of protection against the Severe Acute Respiratory Syndrome CoronaVirus-2, commonly known as
12 COVID-19, infection, has brought unintentional positive side-effects to the country's air quality levels.
13 S5P/TROPOMI monthly mean tropospheric nitrogen dioxide (NO₂) observations show an average decrease of -
14 3% to -26% [-1% to -27%] with an average of -22% [-11%] for March and April 2020 respectively, compared to the
15 previous year, over the six larger Greek metropolitan areas, attributable mostly to vehicular emission reductions.
16 Furthermore, significant effects for shipping emissions over the Aegean Sea as well as the areas surrounding
17 major Greek ports were observed, of approximately -12% [-5%]. For the capital city of Athens, weekly analysis
18 was possible and it revealed a marked decline in NO₂ load between -8% and -43% for seven of the eight weeks
19 studied. Chemical transport modelling, provided by the LOTOS-EUROS CTM, shows that the magnitude of these
20 reductions cannot solely be attributed to the difference in meteorological factors affecting NO₂ levels during
21 March and April 2020 and the equivalent time periods of the previous year. Taking this factor into account, the
22 resulting decline was estimated to range between 0% and -37% for the five largest cities, with an average of ~ -
23 10%. As transport is the second largest sector that affects Greece's air quality, this occasion may well help policy
24 makers in enforcing more targeted measures to aid Greece in further reducing emissions according to
25 international air quality standards.

26 **Keywords:** Air quality; nitrogen dioxide; NO_x; emissions; Sentinel-5P; TROPOMI; LOTOS-EUROS; COVID-19;
27 pandemic; Athens; Greece
28

29 1. Introduction

30 In this work we aim to show the quantifiable and beyond doubt decline in tropospheric nitrogen dioxide
31 (NO₂) levels over Greece during the ongoing Severe Acute Respiratory Syndrome CoronaVirus-2, commonly
32 known as *COVID-19*, pandemic, as sensed by the space-borne S5P/TROPOMI, here after TROPOMI, instrument.
33 By comparing the relative levels for the months of March and April for years 2020 and 2019, while properly
34 accounting for the differences in meteorology using the simulations of a Chemical Transport Model, CTM, we
35 enumerate the improvement in local and regional air quality due to the reduced nitrogen oxides (NO_x) emissions.

36 In the following sections, we provide basic information on tropospheric NO_x, we focus on current knowledge
37 of the nominal NO_x emissions over Greece, we then present a brief overview of the capabilities of current and past
38 satellite instruments in sensing abrupt atmospheric content changes and enumerate the dates when the different
39 lockdown measures were enforced in Greece.

40 1.1. Nitrogen oxides in the troposphere

41 Nitrogen dioxide (NO₂) and nitrogen oxide (NO), referred to more commonly as nitrogen oxides (NO_x), are
42 important trace gases in the Earth's troposphere. NO_x are emitted as a result of both anthropogenic activities, such
43 as fossil fuel combustion and biomass burning, and natural processes, such as microbiological processes in soils,
44 wildfires and lightning. In the presence of sunlight, the photochemical cycle of tropospheric ozone (O₃) converts
45 NO into NO₂ on a timescale of minutes and so NO₂ is considered a robust measure for concentrations of nitrogen
46 oxides (Jacob, 1999). For typical levels of the OH radical, the lifetime of NO_x in the lower troposphere is less than
47 a day, normally a few hours depending on the season and the rates of the photochemical reactions [see for e.g.
48 Beirle et al., 2011; Mijling and van der A, 2012]. As a result, it is well accepted that NO₂ fluxes will remain relatively



49 close to their source which, first of all, makes it possible for NO_x emissions to be well detected from space [see for
50 e.g. Stavrou et al., 2008; Lamsal et al., 2010; van der A et al., 2008, among others] but also precludes any issues
51 of transboundary pollution effects which might otherwise hinder this study.

52 In the troposphere, NO₂ plays a key role in air quality issues, as it directly affects human health [WHO, 2016].
53 In the European Union, the evidence of NO₂ health effects has led to the establishment of air quality standards for
54 the protection of human health. Limit values for NO₂ are set at 200 µg m⁻³ for 1 h average concentrations (with
55 18 exceedances permitted per year), and 40 µg m⁻³ for annual average concentrations (European Council Directive
56 2008/50/EC, 2008). Concentrations above the annual limit value for NO₂ are still widely registered across Europe,
57 even if concentrations and exposures continue to decrease [EEA, 2019]. In Greece in particular, the annual average
58 standard of 40 µg m⁻³ has not been exceeded for years 2007 to 2017 when assuming all in situ stations; the traffic
59 stations of Athens and Thessaloniki however show annual levels up to 45 µg m⁻³ for years 2015 to 2017. It hence
60 follows logically that monitoring closely abrupt changes in NO_x emissions for diverse locations plays a key role in
61 shaping future environmental policies and directives.

62 1.2. Nitrogen dioxide emissions over Greece

63 According to the EEA Report No 8/2019, updated by the EU 2019 Environmental Implementation Review for
64 Greece [EU, 2019], the country's NO_x emissions by sector come from road transport, industry (which mainly covers
65 the energy production and distribution sector), non-road transport, household and agriculture. The relative
66 percentages for NO_x air emissions, separated by sector, as extracted from the 2018 Air Emission Account 2015
67 report by the Hellenic Statistical Authority¹ [HAS, 2018], are: industry 48%, transport 22%, energy supply 18%,
68 manufacturing 6%, central heating 4%, agriculture 1% and others 1%. Based on the European Environmental
69 Agency, EEA, European Pollutant Release and Transfer Register (E-PRTR)², 77% of the reported industrial
70 NO_x/NO₂ emissions over Greece came from thermal power stations and other combustion installations. The
71 monthly energy balance reports³, composed by the Independent Power Transmission Operator of the Hellenic
72 Electricity Transmission System (HETS), show that the total energy requested for March 2020 [4.152GWh] was -
73 2.1% lower than 2019 [4.224GWh], whereas for April 2020 [3.527GWh] was -9.8% lower than 2019 [3.527]. These
74 reductions are quite typical of the seasonality of the energy consumption in Greece which peaks in December and
75 January, due to heating needs, and in July and August, due to cooling needs, with seasonal lows in spring (April
76 and May) and autumn (October and November). Furthermore, in the work of Fameli and Asimakopoulos, 2016, it
77 is reported that the annual mean NO_x emissions for Greece for years 2006 to 2012 can be attributed as follows, in
78 order of relevance: industry, 45±3%, road transport, 35±8%, shipping 11±3%, non-road transport, 10±4%, central
79 heating, 5±2%, with agriculture and aviation showing an average of around 1± each. If we assume that years 2019
80 and 2020 were not exceptional in their temperature levels for the spring months, then it follows that changes in
81 central heating emissions will not bear a significant of the emission changes observed.

82 1.3. Sensing abrupt emission changes from space-borne sensors

83 Abrupt emission changes have already been reported using space-borne observations for a number of recent
84 local and continental circumstances. Castellanos and Boersma, 2012, reported significant reductions in nitrogen
85 oxides over Europe driven by environmental policy and the economic recession based on OMI/Aura observations
86 between 2004 and 2010. Vrekoussis et al., 2013 and Zyrichidou et al., 2019, report strong correlations between
87 pollutant levels and economic indicators showing that the 2008 economic recession has resulted in proportionally
88 lower levels of pollutants in large parts of Greece. The latter, for years 2008 to 2015, showed surprisingly that, while
89 the wintertime tropospheric NO₂ trends were negative, significant positive formaldehyde trends were observed
90 from space, shown to be due to increased usage of affordable indoor heating methods (e.g. fireplaces and wood
91 stoves). Space-sensed reduction in emissions, on a shorter time scale, have also been attributed to strict measures
92 enforced for benign reasons. Mijling et al., 2009, calculated, using OMI/Aura and CTM results, reductions in NO₂
93 concentrations of approximately 60% above Beijing during the 2008 Olympic and Paralympic Games. Ding et al.,

¹ <https://www.statistics.gr/en/statistics/env>

² <https://prtr.eea.europa.eu/#/home>

³ <http://www.admie.gr/en/market-statistics/monthly-energy-balance/>



94 2015, showed a ~30% reduction in OMI/Aura columns, which was translated into a ~25% in actual emission levels
95 during the Nanjing 2014 Youth Olympic Games.

96 Numerous first reports suggesting an improved air quality in after the COVID-19 lockdown was enforced
97 have already been seen in major media outlets. Here we note the findings of Liu et al., 2020, who report, based on
98 both OMI/Aura and TROPOMI, a 48% drop in tropospheric NO₂ from the 20 days averaged before the 2020 Lunar
99 New Year to the 20 days after, which is 20% larger than that from recent years, and relate the increase in decline to
100 the date of each Chinese province lockdown. Bauwens et al., 2020, based on the same sensors, also report an
101 average NO₂ column drop over all Chinese cities of -40% relative to the same period in 2019, while the decreases
102 in Western Europe and the U.S. were found to range between -20 to -38%.

103 1.4. The COVID-19 situation over Greece

104 A short review on the COVID-19 situation over Greece is given here, mainly focusing on providing the dates
105 in March 2020 of the successive restrictive measures that affected NO_x emissions. The country's General Secretariat
106 for Civil Protection, GSVP⁴, reacted quickly to the emerging situation in the neighbouring country Italy and long
107 before the first casualties were reported, major festivities for the Carnival season planned for the 28th of February
108 to the 2nd of March were cancelled, followed by cancellation of all other cultural and sporting activities on March
109 8th. On the 11th of March, all levels of education were suspended, when also a first wave of workplace closures
110 begun and culminated on Monday 16th when all restaurants, cafes with sitting facilities, and in general the food
111 [apart from supermarkets] and hospitality industry were shut down. In the following two days, all remaining retail
112 activities were suspended apart from pharmacies. On Monday 16th restrictions on the size of public gatherings
113 were announced and the public transport section [buses, trams, underground, trains] started to reduce capacity.
114 On the same day, international travel controls began banning incoming flights from high risk countries allowing
115 flights only into Athens International airport, while the four inland borders were shut by the neighbouring
116 countries at the end of March. On Monday 23rd of March, full restrictions on the people's movements were imposed
117 with strict stay-at-home mandates, with exceptions for essential working personnel. The country remained in full
118 lockdown mode until May 4th, including all religious-related congregations, with a complete and without exception
119 restriction around the Greek Orthodox Easter holidays of the 19th of April.

120 These discreet dates of expected change in NO_x emissions permit the analysis and discussion of the
121 observations during this unprecedented period, presented in the results section.

122 2. Materials and Methods

123 In this section we introduce the TROPOMI tropospheric NO₂ observations, the CTM LOTOS-EUROS
124 simulations and the proposed methodology to account for the different meteorological conditions between the
125 nominal period of March-April 2019 and the disrupted one of March-April 2020.

126 2.1. TROPOMI NO₂ observations.

127 The recently launched TROPOMI instrument on the Sentinel-5 Precursor (S5P) mission [Veefkind et al., 2012]
128 has been providing global observations of ozone, nitrogen dioxide, carbon monoxide, sulfur dioxide,
129 formaldehyde, and methane, as well as aerosol and cloud properties⁵ since early 2018. Its very high spatial
130 resolution of 3.5 × 7 km², 3.5 × 5.5 km² since August 2019, and improved signal-to-noise ratio compared to previous
131 space-borne instruments, permits the detection of tropospheric pollution from small-scale emission sources and
132 the estimation of very localized emissions from anthropogenic activities, such as industrial points sources, as well
133 as regional fires. Lorente et al., 2019, have already reported updated emissions over the Paris metropolitan area
134 using TROPOMI observations, while Ialagno et al., 2020, have assessed the capabilities of this instrument in
135 evaluating city-wide air quality levels compared to the more traditional ground-based and in situ NO₂ monitoring
136 methods.

137 In this work we use the publicly available TROPOMI offline v1.2 and v1.3 for March-April 2019 and for March-
138 April 2020 tropospheric NO₂ data accessed via the Copernicus Open Data Access Hub⁶. The algorithm producing

⁴ <https://www.civilprotection.gr/en>

⁵ <http://www.tropomi.eu/>

⁶ <https://scihub.copernicus.eu/>



139 this data is described by van Geffen et al. (2019); it is based on the approach used for processing OMI/Aura NO₂
140 data within DOMINO and the FP7 Quality Assurance for Essential Climate Variables, QA4ECV⁷, projects (Boersma
141 et al, 2011; 2018). Routine validation is being carried out by the Validation Data Analysis Facility⁸, VDAF, who also
142 provide quarterly the Validation Report of the Copernicus Sentinel-5 Precursor Operational Data Products,
143 ROCR-V. Near-real-time validation can also be accessed via the S5P Mission Performance Center Data Validation
144 Server⁹. Here we note that, within the ROCVC #06, reported on the 30th of March 2020, the TROPOMI tropospheric
145 NO₂ columns show a negative bias of roughly -30% compared to global ground-based columnar data, mostly over
146 background regions. Since in this work the relative differences between different time periods will be examined,
147 absolute differences to standard instruments do not affect our findings, as the stability of the TROPOMI datasets
148 is assured.

149 For the purposes of this work, orbital files over Greece, between 19° and 30°E and 34° and 42°N, were gridded
150 onto a 0.10x0.05° grid using the Atmospheric Toolbox¹⁰ for different temporal scenarios discussed below. The
151 data have been filtered, as recommended, using the quality flag indicator ≥ 75 assuring the data under this flag is
152 restricted to cloud-free (cloud radiance fraction < 0.5) and snow-ice free observations. An example figure is
153 presented in Section 3.1 (Figure 2) where the major NO_x emitting sectors around Greece are prominent, the capital
154 city Athens and the second largest city Thessaloniki, in the North, as well as emissions by one of the two largest
155 thermal power plants, in Ptolemaida, also in the North. As in the following we will further discuss the effect on
156 shipping emissions in the Aegean Sea, in the major shipping track that emerges from the Strait of Bosphorus in
157 Istanbul moving SW towards Athens before turning Westwards towards the Mediterranean Sea, the domain also
158 shows emissions from known locations in the Turkish Asia Minor coast, both cities and power plants.

159 For details on the algorithm, as well as the suggested data usage, we refer the reader to the official TROPOMI
160 Algorithm Theoretical Basis Document¹¹, the Product User Manual¹² and the Product Readme File¹³.

161 2.2. LOTOS-EUROS CTM simulations.

162 The open source chemical transport model LOTOS–EUROS¹⁴ v2.2.001 is used for the purposes of this study
163 to simulate NO₂ columns over the Greek domain for March and April for years 2019 and 2020. The CTM model is
164 originally aimed at air pollution studies and simulates gases (O₃, NO_x, SO₂ etc) as well as aerosols (sulfate, nitrate,
165 PM₁₀, PM_{2.5} etc.) in the troposphere. The gas-phase chemistry of the model is a modified version of CBM-IV (Gery
166 et al., 1989). The Isorropia II module (Fountoukis and Nenes, 2007) is used for the aerosol chemistry, while further
167 information on the model and its activity can be found in Manders et al., 2017. LOTOS-EUROS is the national air
168 quality model for the Netherlands (Vlemmix et al., 2015), and has been used for distinct studies as well to
169 investigate NO₂ values (Timmermans et al., 2011; Curier et al., 2012; 2014). LOTOS-EUROS also participates at the
170 operational Copernicus Atmosphere Monitoring Service (CAMS) consisting one of the seven CTMs that provide
171 the official ensemble air quality forecasting service¹⁵.

172 Vlemmix et al., 2015, compared LOTOS-EUROS NO₂ tropospheric columns with MAX-DOAS measurements
173 and found a good agreement between the two datasets, with a correlation coefficient between the daily averaged
174 columns equal to 0.72. Schaap et al., 2013, compared the LOTOS-EUROS NO₂ simulations with OMI/Aura
175 retrievals. They also showed that the model captures the NO₂ spatial distribution satisfactorily and is able to
176 explain 91% of the OMI signal variation across Europe, while the systematic difference was attributed to the
177 summer period. Detailed evaluation of the LOTOS-EUROS NO₂ simulations over Greece have showed that,
178 compared to in situ concentration measurements, the correlation ranges between 0.42 to 0.55 for the different air
179 quality stations studied, while compared to MAXDOAS columns the correlation spans between 0.41 and 0.55 for
180 the urban load and between 0.58 and 0.64 for comparisons over remote directions (Skoulidou et al., 2020.)

181 In this study the domain spans from 19° to 30° East and 34° to 42° North with a grid resolution of 0.1°×0.05°
182 (longitude × latitude), as seen in Figure 1, where an example model NO₂ column output for March 2020 at 12:00

⁷ <http://www.qa4ecv.eu/>

⁸ <http://mpc-vdaf.tropomi.eu/>

⁹ <https://mpc-vdaf-server.tropomi.eu/>

¹⁰ <https://atmospherictoolbox.org/>

¹¹ <http://www.tropomi.eu/document/atbd-nitrogen-dioxide>

¹² <http://www.tropomi.eu/document/product-user-manual-nitrogen-dioxide-0>

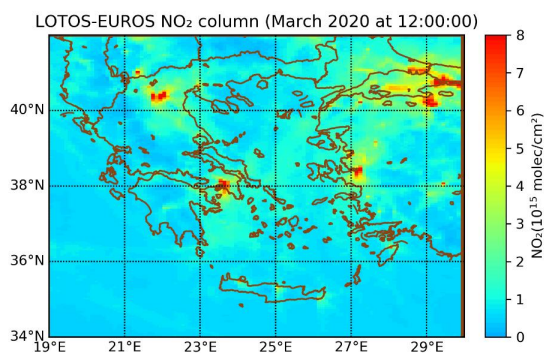
¹³ <http://www.tropomi.eu/document/product-readme-file-nitrogen-dioxide>

¹⁴ <https://lotos-euros.tno.nl/>

¹⁵ <https://www.regional.atmosphere.copernicus.eu/>



183 UTC is shown. The locations of expected emission sources [urban areas, power plants, road transport and shipping
184 plumes] can be seen for the region. In the vertical, the model distinguishes 10 levels which extend from the surface
185 to about 175hPa. The height of these levels refer to the levels of the ECMWF (European Centre for Medium-range
186 Weather Forecasts) meteorological input data that are used to drive the model with an horizontal resolution of
187 7km×7km. The initial and boundary conditions are constrained from a coarser run of LOTOS-EUROS that is
188 performed over the larger European domain (15° W to 45° E and 30° – 60° N) with a resolution of 0.25°×0.25°. The
189 anthropogenic emissions come from the CAMS-REG (CAMS Regional European emissions) inventory for the year
190 2015 with a horizontal resolution of 0.1°×0.05° (Kuenen et al., 2014).



191 Figure 1. Mean LOTOS-EUROS NO₂ tropospheric column in March 2020, at 12Q00 UTC, the approximate overpass time of TROPOMI over the
192 region.

193 2.3. Comparative Methodology.

194 While it would make sense to simply compare the NO₂ levels over Greece for the two periods, assuming that
195 the emission sources have not changed dramatically between 2019 and 2020, one should not discard the effects that
196 various meteorological parameters have on NO₂ levels. Meteorological conditions, such as wind speeds,
197 temperature inversions and the depth of the boundary layer, often play pivotal roles in local air quality levels
198 (Jacob and Winner, 2009). The ambient levels of secondary NO₂ pollution are determined through the accumulation
199 or dispersion of pollutants, low or high solar irradiances, regional transport of clear or polluted air and atmospheric
200 chemistry for the formation of secondary species, in this case via the chemical coupling of NO_x with O₃ (for e.g. Seo
201 et al., 2017).

202 To ensure that the observed decrease in NO₂ levels was not due to diverse meteorological conditions between
203 one year and the next, relative differences on NO₂ columns provided by the LOTOS-EUROS model are calculated
204 and their average magnitude is set as the expected contribution by the different meteorology. This forms a standard
205 level above which we expect COVID-19 related, i.e. emission-related, reductions. The premise of this thinking is as
206 follows: differences in the satellite observations will contain the intertwined effect of differences in meteorology
207 on concentrations and of differences in emissions. For the model we keep the emissions constant for the two periods
208 but use the meteorology of 2019 and 2020 so that we can isolate the impact of meteorology on concentrations. We
209 cannot of course exclude the possibility that the LOTOS-EUROS model has biases in the resulting NO₂ column
210 depending on the meteorological conditions, for example due to uncertainties in mixing under stable conditions,
211 however we expect those to smear out for the spatiotemporal scales studied.

212 In this point we should stress that the satellite observations are more often than not gap-ridden, since in the
213 suggested screening all but clear-skies remain. Spring-time months are rainy months, even for typically sunny
214 Greece, which means that a one-to-one comparison of the satellite observations for the two periods, even on a
215 weekly basis, is usually impossible. During our analysis it was found that, for e.g. the last week of March of 2020,
216 the first week of full lockdown, was fully cloudy for the Northern Greece even though the equivalent week in
217 March 2019 was all sunny. As a result, weekly comparisons were only possible for the major NO₂ hotspot over
218 Greece, the city of Athens, while the rest of the domain was examined on a monthly basis.



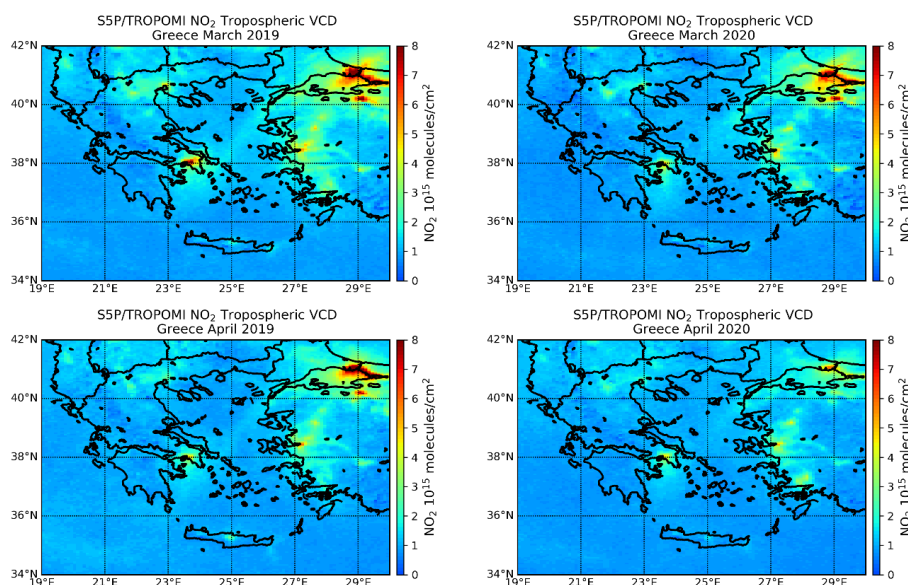
219 In technical terms, the LOTOS-EUROS simulations were performed as discussed in Section 2.2 but for the
220 averaging were restricted, on a daily basis, to the TROPOMI pixels that actually provided an observation. Even
221 though a direct comparison of the CTM results to the satellite data is not the focus of this paper, we imposed this
222 filter to make sure that the same days with the same meteorological conditions were viewed by both methods.
223 Similarly, since we compare the relative changes of the two datasets, and not one against the other, we did not
224 apply the TROPOMI averaging kernels to the CTM profiles, as we would do if we were to directly compare the
225 two.

226 3. Results

227 In the following section, we first show the effect on monthly NO_2 levels over the entire domain, the six Greek
228 cities with the largest number of inhabitants, and on shipping tracks in the Aegean Sea. We then present a more in
229 depth analysis, on a weekly basis, for the city of Athens.

230 3.1. Lockdown effects on monthly NO_2 levels

231 In Figure 2 the monthly mean tropospheric NO_2 levels over Greece, the Northern neighboring countries, the
232 Aegean Sea as well as the coast of Turkey and the Istanbul area, are shown for year 2019 in the left and year 2020
233 in the right, with the month of March presented in the upper panel and the month of April in the lower panel. Even
234 though the hotspots appear strong for year 2019, with discrete shipping tracks and ground-tracks over Turkey
235 showing clearly, the different meteorological conditions between March and April obviously affect both the
236 location of the maxima as well as the absolute level of those maxima. Since Greece entered full lockdown mode
237 within the first three weeks of March, while Turkey imposed intermittent movement restrictions from the
238 beginning of April onwards, the NO_2 hotspot around the megacity of Istanbul and the Bosphorus Strait is still
239 pronounced in March 2020 [upper left] while in Greece most of the smaller urban emission points are missing, and
240 Athens is shown in sharp decline. In April 2020, the Turkish hotspots are also reduced in magnitude, as expected.
241 In the following sections we focus on specific hotspot locations and introduce numerical findings.
242



243 Figure 2. Monthly mean TROPOMI tropospheric NO_2 columns, in 10^{15} molecules/ cm^2 , for March [upper] and April [lower] for
244 the 2019 [left] and 2020 [right].

245

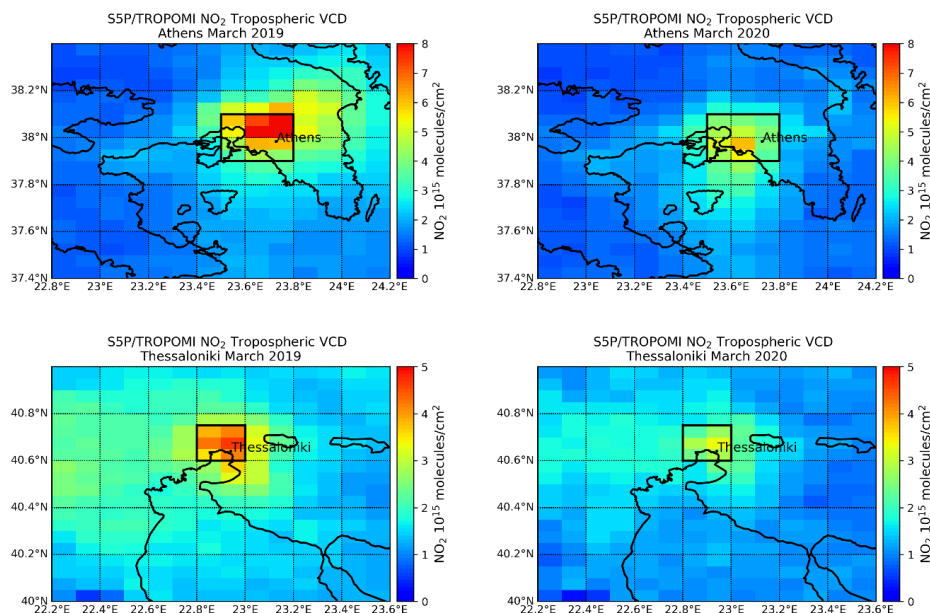


246 Table 1. Geographical distribution and population of the six main cities discussed in this work, as per the 2011
 247 Greek Census.

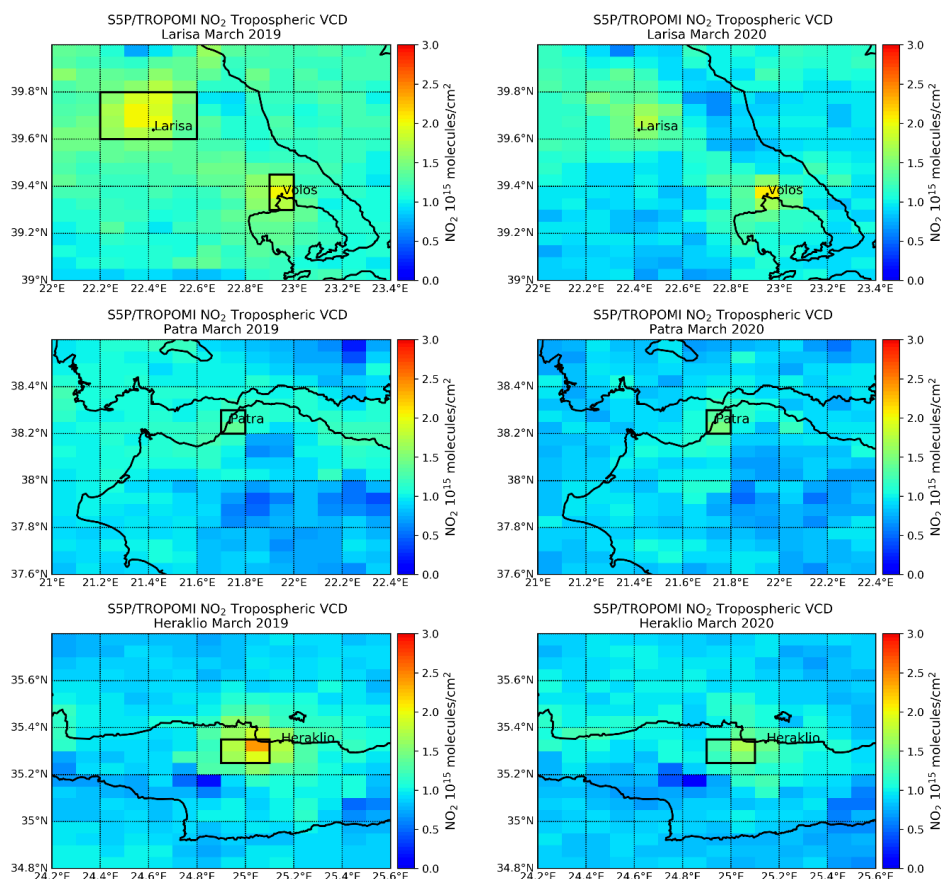
City	Region of	Latitude	Longitude	Population
Athens	Attica	37.98° N	23.72° E	3.218.218
Thessaloniki	Central Macedonia	40.64° N	22.94° E	789.191
Larisa	Thessaly	39.63° N	22.41° E	144.651
Volos	Thessaly	39.36° N	22.95° E	118.707
Patra	Western Greece	38.24° N	21.73° E	168.202
Heraklio	Crete	35.33° N	25.14° E	153.653

248
 249
 250
 251
 252
 253
 254
 255
 256
 257
 258

In Figure 3 the monthly mean TROPOMI tropospheric NO₂ columns, in 10¹⁵ molecules/cm², are depicted for March 2019 [left] and 2020 [right] for six major cities in Greece top to bottom, namely, Athens [37.98° N, 23.72° E], Thessaloniki [40.64° N, 22.94° E], Larisa [39.63° N, 22.41° E], Volos [39.36° N, 22.95° E], Patra [38.24° N, 21.73° E] and Heraklio [35.33° N, 25.14° E]. We focus on the locations where the major transport emissions are expected. These six cities, according to the HAS 2011 census¹⁶, host 4.45 out of the 10.8 million of the Greek population (Table 1). Even though the NO₂ levels are low over the four smaller cities, we were interested in examining the ability of TROPOMI in sensing both the load and expected changes for these, relatively clean, cities [numeric results are given in Table 2].

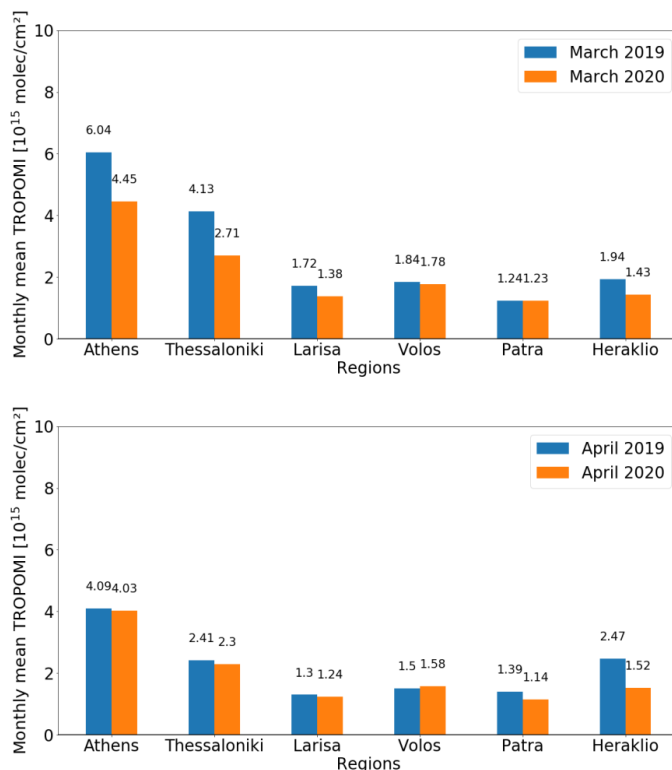


¹⁶ <https://www.statistics.gr/2011-census-pop-hous>



259 Figure 3. Monthly mean TROPOMI tropospheric NO₂ columns, in 10¹⁵ molecules/cm², for March 2019 [left] and March 2020 [right] for the five
260 major cities in Greece. First row, Athens; second, Thessaloniki; third, Larisa and Volos; fourth, Patras and fifth, Heraklio. The boxes mark the
261 pixels used in the numerical analysis.

262
263 In Figure 4 the monthly mean TROPOMI tropospheric NO₂ columns, in 10¹⁵ molecules/cm², for March [upper]
264 and April [lower] for the 2019 [blue] and 2020 [orange] for the six major cities in Greece, from left to right, Athens,
265 Thessaloniki, Larisa, Volos, Patra and Heraklio. Overall, the NO₂ levels are proportional to the city population,
266 with Athens and Thessaloniki showing the highest levels while the remaining four present similar conditions. In
267 Table 2, the full statistics that relate to Figure 4 are given, where it can firstly be noted that for the month of March,
268 the relative differences in NO₂ loading sensed by the satellite sensor between 2019 and 2020 range from -3 to -34%,
269 whereas for the month of April from -1% to -27%, apart from the case of Volos which shows an increase of 5%. In
270 general, as was already seen in Figure 3, the NO₂ levels are higher in all cases for both March months, than the
271 equivalent April ones. Recall as well that, due to the cloudiness conditions, the representability of the months
272 (effective day) is not the same for all cities.
273



274 Figure 4. Monthly mean TROPOMI tropospheric NO₂ columns, in 10¹⁵ molecules/cm², for March [upper] and April [lower] for the 2019 [blue]
 275 and 2020 [orange] for the five major cities in Greece, from left to right, Athens, Thessaloniki, Larisa, Volos, Patra and Heraklio.

276
 277 Table 2. Monthly mean TROPOMI NO₂ levels [10¹⁵ molecules/cm²] over major cities in Greece for March [left block] and April [right block] for
 278 year 2019 and 2020 and their relative difference, standard error and number of pixels [in brackets].

Location	03.2019	03.2020	% diff	04.2019	04.2020	% diff
Athens [12]	6.04±0.48	4.45±0.22	-26%	4.09±0.14	4.03±0.11	-1%
Thessaloniki [6]	4.13±0.14	2.71±0.16	-34%	2.41±0.09	2.30±0.11	-5%
Larisa [6]	1.72±0.06	1.38±0.04	-19%	1.30±0.03	1.24±0.02	-5%
Volos [3]	1.84±0.08	1.78±0.12	-3%	1.50±0.08	1.58±0.11	+5%
Patra [2]	1.24±0.07	1.23±0.06	-	1.39±0.01	1.14±0.01	-18%
Heraklio [4]	2.18±0.14	1.61±0.10	-26%	2.24±0.15	1.64±0.07	-27%

279
 280 As expected, the *in situ* air quality monitoring stations around Athens showed this decrease in a more pronounced
 281 way. Measurements reported in the European Environmental Agency Air Quality monitoring service¹⁷ were
 282 downloaded for stations that reported for both months of March and April 2019 and 2020, namely: two traffic
 283 urban stations (Aristotelous and Patision), two background urban stations (Marousi and Peristeri), an industrial
 284 urban station (Elefsina) and a background suburban station (Agia Paraskeui). The monthly mean surface
 285 concentration [µgr/m³] for March [blue] and April [orange] 2019 and March [grey] and April [yellow] 2020 are

¹⁷ <https://discomap.eea.europa.eu/map/fme/AirQualityExport.htm>



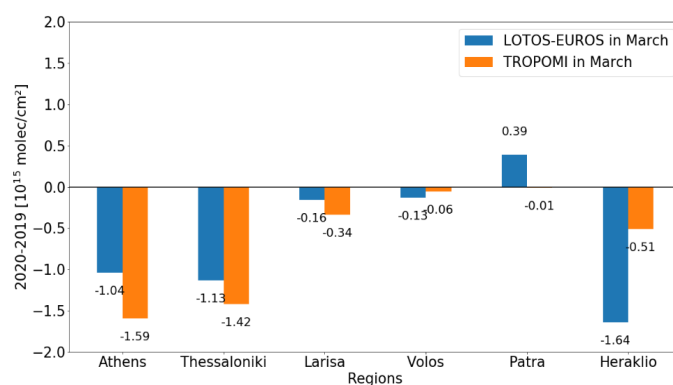
286 shown in Figure S1. The average decrease ranges between ~ -10 and -30% for the entire two month lockdown
287 period, with the lowest variability observed for the case of Elefsina, a station which is mainly affected by the oil
288 refineries and heavy industry. For Thessaloniki, a reduction on surface NO_2 concentrations between -11% and $-$
289 58% between years 2019 and 2020 was reported by the local governing body of the Region of Central Macedonia
290 for the period March 11th to April 20th by the five in situ air quality monitoring stations depending on the type of
291 station, urban suburban and industrial [pers. comm].

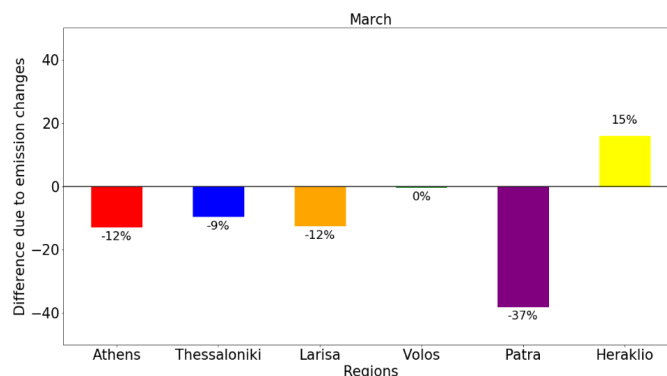
292

293 In Figure 5, upper, the monthly mean absolute differences in tropospheric NO_2 columns (10^{15} molecules/ cm^2)
294 between 2020 and 2019 are shown for TROPOMI [orange] and LOTOS-EUROS [blue] for the five major cities in
295 Greece, for Athens, Thessaloniki, Larisa, Volos, Patra and Heraklio. We opted to show absolute differences here,
296 and not percentage ones as might be expected, since a small relative change on a low NO_2 abundance would result
297 in the erroneous image of a large reduction, as is shown for the case of the city of Patras [second to the right] which
298 also has the lowest reported monthly concentrations, between 1.14 ± 0.01 and $1.39 \pm 0.01 \times 10^{15}$ molecules/ cm^2 for the
299 months shown. In the lower panel of Figure 5, the emission changes are quantified in the following manner: the
300 percentage differences for LOTOS-EUROS between 2019 and 2020 are calculated, as the equivalent ones seen by
301 TROPOMI. By subtracting the two percentage differences, and not directly comparing the two, the actual NO_2
302 reduction may be quantified. This is roughly be -12% for Athens, -9% for Thessaloniki, -12% for Larisa, near zero
303 for Volos [as was already seen by the TROPOMI observations, Figure 3, third panel], -37% for Patra and
304 unexpectedly positive, $+15\%$, for Heraklio.

305

306



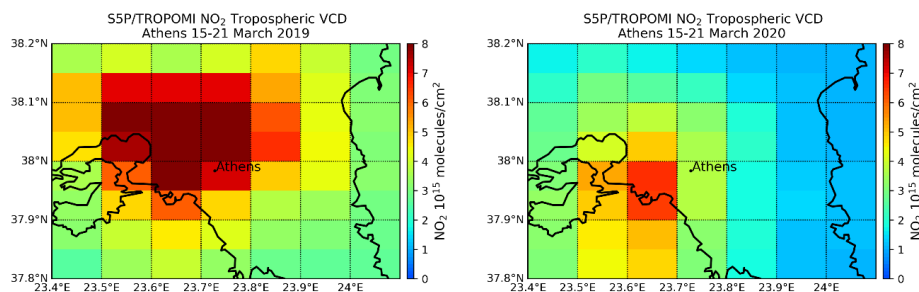


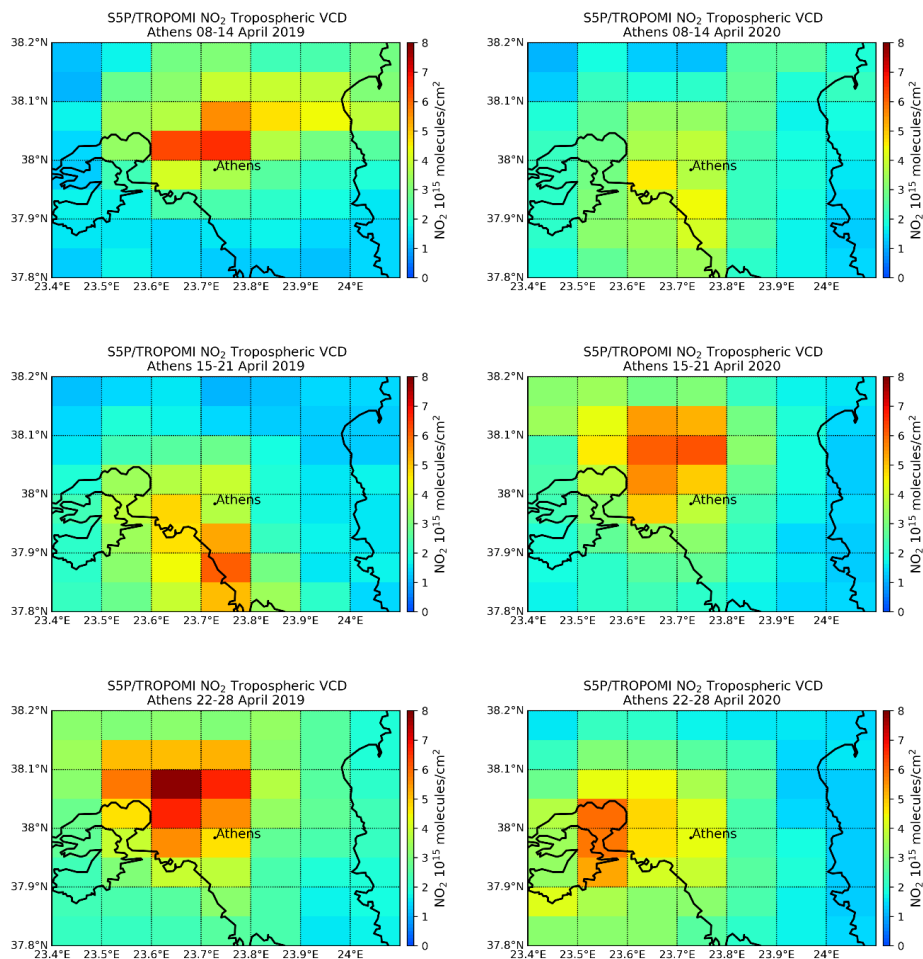
307 Figure 5. Upper. Monthly mean absolute differences in tropospheric NO_2 columns (10^{15} molecules/ cm^2) between 2020 and 2019 are shown for
308 TROPOMI [orange] and LOTOS-EUROS [blue] for the five major cities in Greece, from left to right, Athens, Thessaloniki, Larisa, Volos, Patra
309 and Heraklio. Lower. The percentage differences attributed to emission changes.

310

311 Apart from the reduction in NO_x emissions due to land transport restrictions, some decline is also expected in
312 shipping emissions over the Aegean Sea routes. In Figure S2 the land is masked so as to reveal the shipping tracks
313 between the Bosphorus Strait and the port of Piraeus in Athens for March 2019 [left] and March 2020 [right.]
314 Excluding the background values over the open sea, we calculate a monthly mean of 1.50×10^{15} molecules/ cm^2 for
315 2019 compared to 1.32×10^{15} molecules/ cm^2 for 2020, a -12% [-5% for April] reduction, well in line with the reductions
316 found over land.

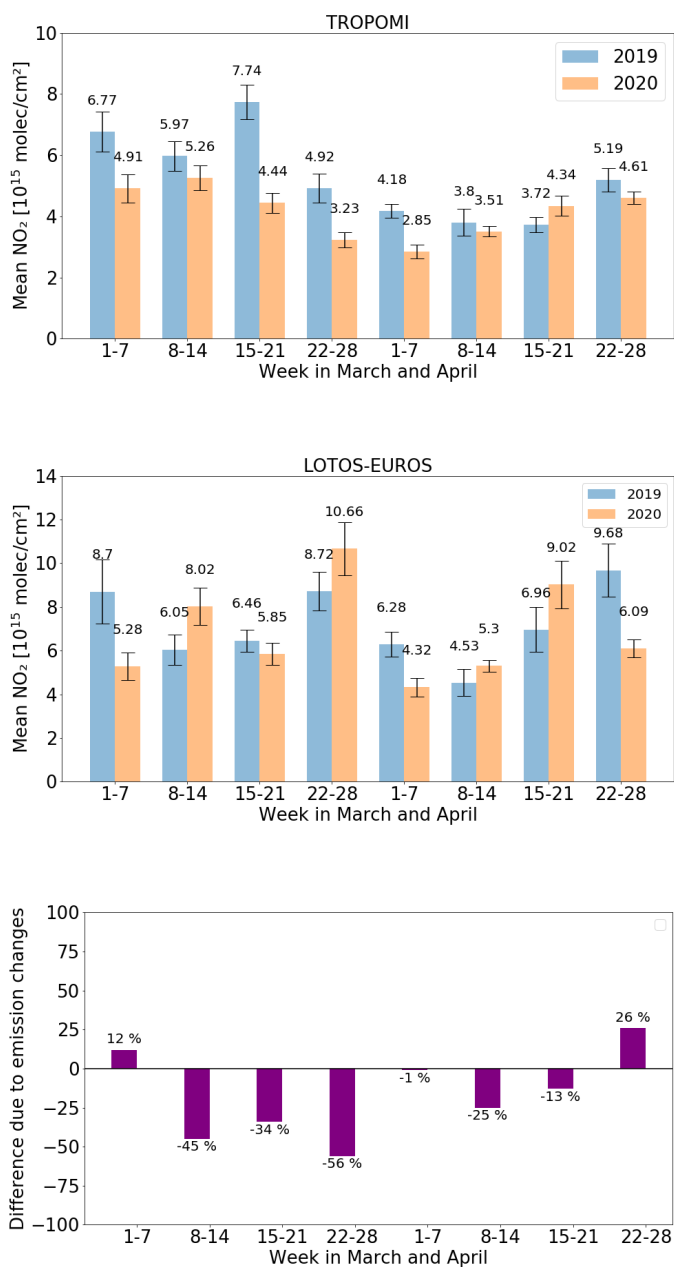
317 3.2. Lockdown effects on weekly NO_2 levels over Athens





318 Figure 6. Weekly mean TROPOMI tropospheric NO₂ columns, in 10¹⁵ molecules/cm², over Athens for 2019 [left] and 2020 [right]. First row, 15-
319 21 March 2019; second, 8-14 April, third, 15-21 April and fourth, 22-28 April.

320



321 Figure 7. Upper. Weekly mean TROPOMI tropospheric NO₂ columns, in 10¹⁵ molecules/cm², for weeks in the 2019 [blue] and 2020 [orange] for
 322 Athens. Middle. Weekly mean LOTOS-EUROS tropospheric NO₂ columns, in 10¹⁵ molecules/cm², for weeks in the 2019 [blue] and 2020 [orange]
 323 for Athens. Lower Lower. The percentage differences attributed to emission changes, revealing the actual magnitude of the NO_x emissions
 324 decrease.



325 Without disregarding the possible contribution of central heating to total NO_x emissions, the largest decrease due
326 to the COVID-19 lockdown is indeed observed over the main Greek hotspot, the city of Athens and its surrounding.
327 In Figure 6, weekly mean TROPOMI tropospheric NO₂ columns, in 10¹⁵ molecules/cm², over Athens for 2019 [left]
328 and 2020 [right] are shown for weeks 15-21 March (first row), 8-14 April (second row), 15-21 April (third row) and
329 22-28 April (fourth row). Apart from the obvious reduction in magnitude this year, what is most prominent in this
330 composite is the effect of the winds for both the location of the local maximum as well as the spread of the pollution
331 plume, which further strengthens our decision not to perform one-on-one comparisons between the different NO₂
332 fields. In numbers, the average weekly NO₂ load over Athens sensed by TROPOMI is presented in the upper panel
333 of Figure 7 where the 2019 averages are shown in blue and the 2020 ones in orange for weeks of March and April.
334 Out of the 12 pixels considered for this sub-domain, which may give up to 84 measurements for each week, for
335 year 2019 an average of 53±16 [median of 52] S5P/TROPOMI observations were found whereas for year 2020 an
336 average of 52±25 [median of 56]. Even though the representativeness of the weekly levels can by no means be
337 considered equal between the years, apart from the penultimate week, TROPOMI reports lower NO₂ columns
338 ranging between -8% to -43%. The contribution of the meteorological factors to these estimates can be assessed by
339 the equivalent LOTOS-EUROS weekly averages, shown in the middle panel of Figure 7. As for Figure 5, bottom,
340 the percentage difference of the LOTOS-EUROS simulations between 2019 and 2020 are calculated, as those for
341 TROPOMI. The difference between those two relative differences is given in the lower panel of Figure 7. The fact
342 that the CTM predicted an increase in NO₂ production for most weeks, under the assumption that the primary
343 emissions remained stable between the two years, results in higher reduction levels ranging between -1% to -56%.

344 4. Conclusions

345 In this work, Sentinel-5P/TROPOMI tropospheric NO₂ observations were studied in order to examine the
346 possible positive effect on Greek air quality caused the recent COVID-19 pandemic lockdown. The country
347 enforced severe movement restrictions and entire economic sectors gradually were shut down, starting from the
348 last weekend of February and gradually, activity per activity, reaching a total lockdown in effect from Monday 23rd
349 up to May 4th. The time period between March and April 2020, and the equivalent weeks in 2019, were analyzed
350 and compared for six, largest in population, cities in Greece, as well as the shipping lanes of the Aegean Sea.
351 TROPOMI monthly mean tropospheric nitrogen dioxide, NO₂, observations showed a decrease of between -3%
352 and -26% [-1% to -27%] with an average of -22% [-11%] for March and April 2020 respectively, compared to the
353 previous year, for the urban areas and approximately -12% [-5%] for the shipping sector. For the capital city of
354 Athens, weekly reductions, between -8% and -43%, for the seven of the eight weeks studied were found. Similar
355 reductions were reported by six in situ air quality stations in Athens that reported measurements to the European
356 Environmental Agency Air Quality database, with monthly decreases ranging between 0% to -47% and an average
357 of -23%. In order to eliminate the expected meteorological effects on the observed NO₂ levels, Chemical Transport
358 Modelling simulations, provided by the LOTOS-EUROS CTM, show that the magnitude of these satellite-sensed
359 reductions cannot solely be attributed to the difference in meteorological factors affecting NO₂ levels during March
360 and April 2020 and the equivalent time periods of the previous year. Taking this factor into account, the resulting
361 decline due to the COVID-19 related measures was estimated to range between 0% and -37% for the five largest
362 Greek cities, with an average of ~ -10%.

363 **Author Contributions:** The data analysis was performed by A.K., I.S. and M.E.K.; methodology and conceptualization by D.S.
364 and I.P.; software development by I.S. and A.K.; writing—original draft preparation by M.E.K.; review and editing by D.S.,
365 A.S., A.M., J.v.G. and H.E. All authors have read and agreed to the published version of the manuscript.

366 **Funding:** This research has been co-financed by the European Union (European Regional Development Fund) and Greek
367 national funds through the Operational Program “Competitiveness, Entrepreneurship and Innovation” (NSRF 2014-2020) by
368 the “Panhellenic Infrastructure for Atmospheric Composition and Climate Change” project (MIS 5021516) and well as the



369 “Innovative system for Air Quality Monitoring and Forecasting” project [code T1EDK-01697, MIS 5031298], implemented under
370 the Action “Reinforcement of the Research and Innovation” Infrastructure.

371 **Acknowledgments:** We acknowledge the usage of modified Copernicus Sentinel data 2019-2020. Results presented in this work
372 have been produced using the Aristotle University of Thessaloniki (AUTH) High Performance Computing Infrastructure and
373 Resources. M.E.K., I.S. and D.S. would like to acknowledge the support provided by the IT Center of the AUTH throughout the
374 progress of this research work. M.E.K. and A.K. would also like to acknowledge the support provided by the Atmospheric
375 Toolbox@.

376 **Conflicts of Interest:** The authors declare no conflict of interest.

377 **Data availability:** The S5P/TROPOMI data are publicly available via the Copernicus Open Data Access Hub,
378 <https://scihub.copernicus.eu/>. The LOTOS-EUROS simulations are available upon request. The air quality monitoring station
379 data are publicly available via the European Environmental Agency Air Quality monitoring service,
380 <https://discomap.eea.europa.eu/map/fme/AirQualityExport.htm>.

381 References

- 382 Bauwens, M., Compennolle, S., Stavrakou, T., Müller, J.-F., van Gent, J., Eskes, H., et al. (2020) Impact of coronavirus outbreak
383 on NO₂ pollution assessed using TROPOMI and OMI observations. *Geophysical Research Letters*, 47,
384 e2020GL087978. <https://doi.org/10.1029/2020GL087978>
- 385 Beirle, S., Boersma, K. F., Platt, U., Lawrence, M. G., and Wagner, T. (2011). Megacity emissions and lifetimes of nitrogen oxides
386 probed from space. *Science*, 333:1737–1739, DOI: 10.1126/science.1207824.
- 387 Schaub, D., Brunner, D., Boersma, K. F., Keller, J., Folini, D., Buchmann, B., Berresheim, H., and Staehelin, J.: SCIAMACHY
388 tropospheric NO₂ over Switzerland: estimates of NO_x lifetimes and impact of the complex Alpine topography on the retrieval,
389 *Atmos. Chem. Phys.*, 7, 5971–5987, <https://doi.org/10.5194/acp-7-5971-2007>, 2007.
- 390 Boersma, K. F., Eskes, H. J., Dirksen, R. J., van der A, R. J., Veefkind, J. P., Stammes, P., Huijnen, V., Kleipool, Q. L., Sneep, M.,
391 Claas, J., Leitão, J., Richter, A., Zhou, Y., and Brunner, D.: An improved tropospheric NO₂ column retrieval algorithm for the
392 Ozone Monitoring Instrument, *Atmos. Meas. Tech.*, 4, 1905–1928, <https://doi.org/10.5194/amt-4-1905-2011>, 2011.
- 393 Boersma, K. F., Eskes, H. J., Richter, A., De Smedt, I., Lorente, A., Beirle, S., van Geffen, J. H. G. M., Zara, M., Peters, E., Van
394 Roozendaal, M., Wagner, T., Maasakkers, J. D., van der A, R. J., Nightingale, J., De Rudder, A., Irie, H., Pinardi, G., Lambert, J.-
395 C., and Compennolle, S. C.: Improving algorithms and uncertainty estimates for satellite NO₂ retrievals: results from the quality
396 assurance for the essential climate variables (QA4ECV) project, *Atmos. Meas. Tech.*, 11, 6651–6678, [https://doi.org/10.5194/amt-](https://doi.org/10.5194/amt-11-6651-2018)
397 11-6651-2018, 2018.
- 398 Castellanos, P., Boersma, K. Reductions in nitrogen oxides over Europe driven by environmental policy and economic recession.
399 *Sci Rep* 2, 265 (2012). <https://doi.org/10.1038/srep00265>
- 400 Curier, R. L., R. Kranenburg, A.J.S. Segers, R.M.A. Timmermans, M. Schaap, Synergistic use of OMI NO₂ tropospheric columns
401 and LOTOS-EUROS to evaluate the NO_x emission trends across Europe, *Remote Sensing of Environment*, 149, 2014, 58–69,
402 <https://doi.org/10.1016/j.rse.2014.03.032>.
- 403 Curier, R. L., R. Timmermans, S. Calabretta-Jongen, H. Eskes, A. Segers, D. Swart, M. Schaap, Improving ozone forecasts over
404 Europe by synergistic use of the LOTOS-EUROS chemical transport model and in-situ measurements, *Atmospheric*
405 *Environment*, 60, 2012, 217–226, <https://doi.org/10.1016/j.atmosenv.2012.06.017>.
- 406 Daniel J. Jacob and Darrell A. Winner, Effect of climate change on air quality, *Atmospheric Environment*, Volume 43, Issue 1,
407 Pages 51–63, <https://doi.org/10.1016/j.atmosenv.2008.09.051>, 2009.
- 408 Ding, J., van der A, R. J., Mijling, B., Levelt, P. F., and Hao, N.: NO_x emission estimates during the 2014 Youth Olympic Games
409 in Nanjing, *Atmos. Chem. Phys.*, 15, 9399–9412, <https://doi.org/10.5194/acp-15-9399-2015>, 2015.
- 410 European Environmental Agency, EEA: Air quality in Europe – 2019 report, doi:10.2800/822355, available at:
411 <https://www.eea.europa.eu/publications/air-quality-in-europe-2019>, last access: 29.04.2020.
- 412 European Environmental Agency, EEA: Report No 8/2019, European Union emission inventory report 1990-2017 under the
413 UNECE Convention on Long-range Transboundary Air Pollution (LRTAP), doi:10.2800/78220, available at:
414 <https://www.eea.europa.eu/publications/european-union-emissions-inventory-report-2017>, last access: 29.04.2020
- 415 European Union, EU: The Environmental Implementation Review 2019, COUNTRY REPORT: GREECE, available at
416 https://ec.europa.eu/environment/eir/pdf/report_el_en.pdf, last access: 30.04.2020
- 417 Fameli, K.M. and V.D. Assimakopoulos, Development of a road transport emission inventory for Greece and the Greater Athens
418 Area: Effects of important parameters, *Science of The Total Environment*, 505, 2015, 770–786,
419 <https://doi.org/10.1016/j.scitotenv.2014.10.015>.



- 420 Fountoukis, C. and Nenes, A.: ISORROPIA II: a computationally efficient thermodynamic equilibrium model for K^+ - Ca^{2+} - Mg^{2+} -
421 NH_4^+ - Na^+ - SO_4^{2-} - NO_3^- - Cl^- - H_2O aerosols, *Atmos. Chem. Phys.*, 7, 4639–4659, <https://doi.org/10.5194/acp-7-4639-2007>, 2007.
- 422 Georgoulas, A. K., van der A, R. J., Stammes, P., et al., Trends and trend reversal detection in 2 decades of tropospheric NO_2
423 satellite observations, *Atmos. Chem. Phys.*, 19, 6269–6294, <https://doi.org/10.5194/acp-19-6269-2019>, 2019.
- 424 Gery, M. W., Whitten, G. Z., Killus, J. P., and Dodge, M. C. (1989), A photochemical kinetics mechanism for urban and regional
425 scale computer modeling, *J. Geophys. Res.*, 94(D10), 12925–12956, doi:[10.1029/JD094iD10p12925](https://doi.org/10.1029/JD094iD10p12925).
- 426 Hellenic Statistical Authority, HAS: Air Emission Accounts, 2015, available at <https://www.statistics.gr/en/statistics/-/publication/SOP08/>, 2018, last access: 30.04.2020
- 427 Ialongo, I., Virta, H., Eskes, H., Hovila, J., and Douros, J.: Comparison of TROPOMI/Sentinel-5 Precursor NO_2 observations with
428 ground-based measurements in Helsinki, *Atmos. Meas. Tech.*, 13, 205–218, <https://doi.org/10.5194/amt-13-205-2020>, 2020.
- 430 Jacob, D. J. (1999). Introduction to Atmospheric Chemistry. Princeton University Press, ISBN-10: 0691001855.
- 431 Kuenen, J. J. P., Visschedijk, A. J. H., Jozwicka, M., and Denier van der Gon, H. A. C.: TNO-MACC_II emission inventory; a
432 multi-year (2003–2009) consistent high-resolution European emission inventory for air quality modelling, *Atmos. Chem. Phys.*,
433 14, 10963–10976, <https://doi.org/10.5194/acp-14-10963-2014>, 2014.
- 434 Lamsal, L. N., Martin, R. V., van Donkelaar, A., Celarier, E. A., Bucsela, E. J., Boersma, K. F., Dirksen, R., Luo, C., and Wang,
435 Y. (2010), Indirect validation of tropospheric nitrogen dioxide retrieved from the OMI satellite instrument: Insight into the
436 seasonal variation of nitrogen oxides at northern midlatitudes, *J. Geophys. Res.*, 115, D05302, doi:[10.1029/2009JD013351](https://doi.org/10.1029/2009JD013351).
- 437 Liu, Fei, Aaron Page, Sarah A. Strode, Yasuko Yoshida, Sungyeon Choi, Bo Zheng, Lok N. Lamsal, Can Li, Nickolay A. Krotkov,
438 Henk Eskes, Ronald van der A, Pepijn Veefkind, Pieternel Levelt, Joanna Joiner, Oliver P. Hausser, Abrupt declines in
439 tropospheric nitrogen dioxide over China after the outbreak of COVID-19, preprint, <https://arxiv.org/abs/2004.06542>, 2020.
- 440 Lorente, A., Boersma, K.F., Eskes, H.J. et al. Quantification of nitrogen oxides emissions from build-up of pollution over Paris
441 with TROPOMI. *Sci Rep* 9, 20033 (2019). <https://doi.org/10.1038/s41598-019-56428-5>.
- 442 Manders, A. M. M., Builtjes, P. J. H., Curier, L., Denier van der Gon, H. A. C., Hendriks, C., Jonkers, S., Kranenburg, R., Kuenen,
443 J. J. P., Segers, A. J., Timmermans, R. M. A., Visschedijk, A. J. H., Wichink Kruit, R. J., van Pul, W. A. J., Sauter, F. J., van der
444 Swaluw, E., Swart, D. P. J., Douros, J., Eskes, H., van Meijgaard, E., van Ulft, B., van Velthoven, P., Banzhaf, S., Mues, A. C.,
445 Stern, R., Fu, G., Lu, S., Heemink, A., van Velzen, N., and Schaap, M.: Curriculum vitae of the LOTOS-EUROS (v2.0) chemistry
446 transport model, *Geosci. Model Dev.*, 10, 4145–4173, <https://doi.org/10.5194/gmd-10-4145-2017>, 2017.
- 447 Mijling, B., and van der A, R. J. (2012), Using daily satellite observations to estimate emissions of short-lived air pollutants on a
448 mesoscopic scale, *J. Geophys. Res.*, 117, D17302, doi:[10.1029/2012JD017817](https://doi.org/10.1029/2012JD017817).
- 449 Mijling, B., R. van der A, K. Boersma, M. Van Roozendaal, I. De Smedt, and H. Kelder (2009). Reductions of NO_2 detected from
450 space during the 2008 Beijing Olympic Games. *Geophys. Res. Lett.* 36, L13801.
- 451 S5P MPC Routine Operations Consolidated Validation Report (ROCVR), Quarterly Validation Report of the Copernicus
452 Sentinel-5 Precursor Operational Data Products #06: April 2018 – February 2020, S5P-MPC-IASB-ROCVR-06.0.1-20200330,
453 http://mpc-vdaf.tropomi.eu/ProjectDir/reports/pdf/S5P-MPC-IASB-ROCVR-06.0.1-20200330_FINAL.pdf, eds: J.-C. Lambert
454 and A. Keppens, issue number: version 06.0.1, 2020-03-30.
- 455 Schaap M, Kranenburg R, Curier L, Jozwicka M, Dammers E, Timmermans R. Assessing the Sensitivity of the OMI- NO_2 Product
456 to Emission Changes across Europe. *Remote Sensing*. 2013; 5(9):4187-4208, <https://doi.org/10.3390/rs5094187>
- 457 Skoulidou, I., M. E. Koukouli, A. Manders, A. Segers, D. Karagiokizidis, M. Gratsea, D. Balis, A. Bais, T. Stavrou, J. Van Geffen
458 and H. Eskes, Evaluation on LOTOS-EUROS NO_2 simulations using ground-based measurements and S5P/TROPOMI
459 observations over Greece, in submission to ACPD, 2020.
- 460 Seo, J., Kim, J. Y., Youn, D., Lee, J. Y., Kim, H., Lim, Y. B., Kim, Y., and Jin, H. C.: On the multiday haze in the Asian continental
461 outflow: the important role of synoptic conditions combined with regional and local sources, *Atmos. Chem. Phys.*, 17, 9311–
462 9332, <https://doi.org/10.5194/acp-17-9311-2017>, 2017.
- 463 Stavrou, T., Müller, J.-F., Boersma, K. F., De Smedt, I., and van der A, R. J. (2008), Assessing the distribution and growth rates
464 of NO_2 emission sources by inverting a 10-year record of NO_2 satellite columns, *Geophys. Res. Lett.*, 35, L1801,
465 doi:[10.1029/2008GL033521](https://doi.org/10.1029/2008GL033521).
- 466 van der A, R. J., Eskes, H. J., Boersma, K. F., van Noije, T. P. C., Van Roozendaal, M., De Smedt, I., Peters, D. H. M. U., and
467 Meijer, E. W. (2008), Trends, seasonal variability and dominant NO_x source derived from a ten year record of NO_2 measured
468 from space, *J. Geophys. Res.*, 113, D04302, doi:[10.1029/2007JD009021](https://doi.org/10.1029/2007JD009021).
- 469 van Geffen, J. H. G. M., Eskes, H. J., Boersma, K. F., Maasackers J. D. and Veefkind, J. P., TROPOMI ATBD of the total and
470 tropospheric NO_2 data products, Report S5P-KNMI-L2-0005-RP, version 1.4.0, released 6 Feb. 2019, KNMI, De Bilt, The
471 Netherlands, available at <http://www.tropomi.eu/documents/atbd/>, last access: 08 May 2020.



472 Veefkind, J. P. et al. TROPOMI on the ESA Sentinel-5 Precursor: A GMES mission for global observations of the atmospheric
473 composition for climate, air quality and ozone layer applications. *Rem. Sens. Env.* 120, 70–83 (2012),
474 <https://doi.org/10.1016/j.rse.2011.09.027>.
475 Vlemmix, T., Eskes, H. J., Piters, A. J. M., Schaap, M., Sauter, F. J., Kelder, H., and Levelt, P. F.: MAX-DOAS tropospheric nitrogen
476 dioxide column measurements compared with the Lotos-Euros air quality model, *Atmos. Chem. Phys.*, 15, 1313–1330,
477 <https://doi.org/10.5194/acp-15-1313-2015>, 2015.
478 Timmermans R., Eskes H., Builtjes P., Segers A., Swart D., Schaap M. (2011) LOTOS-EUROS Air Quality Forecasts by
479 Assimilation of OMI Tropospheric NO₂ Columns. In: Steyn D., Trini Castelli S. (eds) *Air Pollution Modeling and its Application*
480 *XXI NATO Science for Peace and Security Series C: Environmental Security*. Springer, Dordrecht.
481 Vrekoussis, M., Richter, A., Hilboll, A., et al., Economic Crisis Detected from Space: Air Quality observations over
482 Athens/Greece, *Geophys. Res. Lett.*, 40, 458–463, <https://doi.org/10.1002/grl.50118>, 2013.
483 World Health Organization, WHO: *Ambient air pollution: A global assessment of exposure and burden of disease*, World
484 Health Organisation, ISBN: 9789241511353, Bonn, 2016.
485 Zyrichidou, I., D. Balis, M.E. Koukouli, et al., Adverse results of the economic crisis: A study on the emergence of enhanced
486 formaldehyde (HCHO) levels seen from satellites over Greek urban sites, *Atmospheric Research*,
487 <https://doi.org/10.1016/j.atmosres.2019.03.017>, 2019.
488



© 2020 by the authors. Submitted for possible open access publication under the terms
and conditions of the Creative Commons Attribution (CC BY) license
(<http://creativecommons.org/licenses/by/4.0/>).

489